doi:10.3788/gzxb20144310.1006002

连续变量相干光通信中的联合调制编码系统

黄春晖,万君
(福州大学 物理与信息工程学院,福州 350116)

摘 要:根据单束光连续变量相干光通信的编码要求,提出一种联合磁光调制和电光调制的联合调制系统;根据 Stokes 参量与邦加球的映射关系以及 Stokes 矩阵理论,分析了该系统的编码原理,构造了单光束相干光通信系统,并根据编码的需要设计了相关的磁光调制器驱动控制电路和随机数产生电路.最后利用零差检测技术测量 Stokes 参量;将发送码与接收码进行整形处理后,得到误码率小于 3.60%的通信效果,证明了该联合调制实验方案的可行性.为连续变量密钥分配提供一种简捷的编码方法.

关键词:相干光通信;联合调制编码;连续变量;量子密钥分配
中图分类号:TN918 **文献标识码**:A **文章编号**:1004-4213(2014)10-1006002-7

System of Joint Modulation Code in Continuous Variable Coherent Optical Communication

HUANG Chun-hui, WAN Jun
(*College of Physics and Information Engineering, Fuzhou University, Fuzhou* 350106, *China*)

Abstract: Based on the encoding requirements of the continuous variable coherent optical communication in the single beam light, a novel encoding scheme by the joint modulation including magneto-optic modulation and electro-optic modulation was proposed. According to the mapping relationship between Stokes parameters and Poincare sphere, the coding principle of the joint modulation is analyzed in Stokes matrix theory. Then a single beam optical system is set up for encoding. And based on the needs of encoding, a driving circuit of magneto-optic modulatior and a circuit of random number generator are designed. By homodyne detection technique, the Stokes parameters are measured, and the error rate is estimated by LabVIEW procedure. The raw data show that the error rate is lower than 3.60%, which verify the feasibility of the encoding scheme.

Key words: Coherent optical communication; Joint modultion; Continous variable; Quantum key distribution
OCIS Codes: 060.1660; 060.4080; 030.1640; 270.1670

0 Introduction

Quantum Key Distribution (QKD) is the core technology of quantum cryptography. Currently, the information carrier of QKD includes single photon [1-2] and a certain intensity of coherent light [3-4]. However, there are some obstacles on the preparation of single photon, such as complicated production process and high manufacture cost, while coherent light interest many people [5-6] in the world, because of the advantages of long transmission distance, high sensitivity, diverse modulation methods, and so on. Continuous Variable Quantum Key Distribution (CVQKD) is one of them, it can be divided into two types in terms of light path structure: two-beams and single-beam. CVQKD in two-beam has drawn much attention around the world since Grangier realized it in 2003 [7]. However, there are still several difficulties: 1) Local Oscillator (LO) light and the signal light must be sufficiently close to each other for interfering; 2) The propagation direction of beams

Foundation item: The National Natural Science Foundation of China (No. 61177072)
First author: HUANG Chun-hui (1959—), male, professor, mainly focuses on quantum communication and integrated circuit. Email: hchfzu@163.com
Received: Jan. 08, 2014; **Accepted**: Mar. 25, 2014

in free space may changes at any time due to the scattering, and any actual microvibration would affect the accuracy of measurement; 3) The signal light and LO are hard to keep synchronized when they propagate for a long distance; 4) The tracking control procedure is usually very complex on the reason of the hysteresis and creep nonlinearities of Piezoelectric Transducer (PZT). Nevertheless, Compared with two-beam, the single-beam is a new optical communication developed in recent years, which contains LO component and signal component [8], so not only does it simplify the optical communication system, but it can overcome the difficulty of synchronization between the local light and the signal light[9-10].

In this paper, based on the characteristics of Electro-Optic Modulator (EOM) and Magneto-Optic Modulator (MOM), a joint modulation scheme for single-beam CVQKD in free space was proposed; then set up a communication system including sending and detecting for demonstrating our scheme, besides design a driving circuit of MOM and a random number generator; finally a LabVIEW was programed procedure to control data acquisition and analyze the collected data.

1 Structure and principle of the system

Our system is shown in Fig. 1 which can be divided into the following four parts: 1) a laser source generates coherent light beam and then the beam is purified as one horizontal polarized light by a polarizer and PBS; 2) the encoding system consisting of a MOM and a EOM; 3) A optical detection system consists of a wave plate and a photoelectric detection circuit. 4) an analysis system for processing of measurement results, it consists of a LabVIEW platform and a data acquisition card.

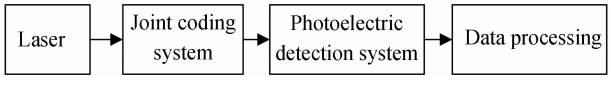

Fig. 1 Block diagram of experimental system

Generally, CVQKD is closely related to polarization state generator which is mainly classified as electro-optic amplitude modulator, electro-optic phase modulator, magneto-optic modulator and fiber extrusion modulator. The EOM requires higher bias voltage and generates great loss; Magneto-optic modulation is difficult to implement the encoding of two orthogonal components; As for the fiber extrusion modulator, it's more complex to implement algorithms and circuits. In this paper, based on the characteristics of EOM and MOM, a joint modulation scheme is proposed, and not only dose it avoid the weaknesses described above, but it is more convenient to realize. The results of experiment show that the scheme can meet the requirement of single-beam continuous variable quantum coherent optical communications.

In order to specify communication process, Stokes parameters are introduced to describe any partial or a complete polarized light, The polarized light consists of four parameters of Stokes: S_0, S_1, S_2, S_3, each parameter has its physical meaning. Therefore, we can obtain the useful information by detecting the parameters of Stokes. For complete polarized light, Stokes parameters satisfy with $S_0^2=S_1^2+S_2^2+S_3^2$. To be more convenient for measuring, S_2 or S_3 is selected as QKD in this paper.

2 Encoding of S_2 and S_3

The optical system of CVQKD in our scheme is shown in Fig. 2. Considering the 808 nm light is within the optimal window air transport [11], while generally atmospheric loss window is very low (<0.1 dB/km) and under atmospheric conditions, the laser source (SDK5412) is selected, it satisfies the requirement of free space transmission in the free space. Then a pure quasi-parallel beam is obtained, in turn, through the lens and isolator, the beam splitter and the polarizing plate. The completely polarized light beam can be obtained, after a partial purification which can be expressed as: $\boldsymbol{E}_i=(E_x \quad 0)^{\mathrm{T}}$.

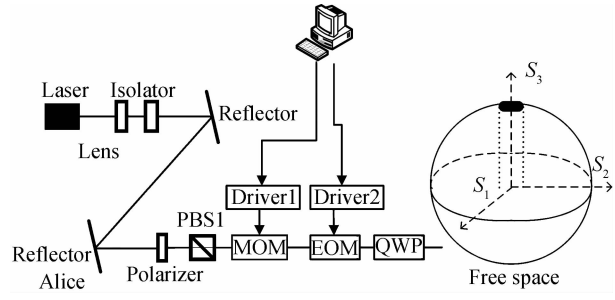

Fig. 2 Schematic diagram of encoding S_2

Then, the horizontal polarized light beam is encoded by a joint modulation system consisting of MOM and EOM .

According to Jones theory, the function of MOM can be described by

$$\boldsymbol{P}_{\mathrm{MOM}}=\begin{pmatrix}\cos\theta & -\sin\theta\\ \sin\theta & \cos\theta\end{pmatrix} \tag{1}$$

where θ represents the rotation angle of the polarized light; The EOM is equivalent to a wave plate whose phase is variable, it consists of two orthogonal crystals [12], so the action of EOM is presented as

$$\boldsymbol{P}_{\mathrm{EOM}}=\begin{pmatrix}\mathrm{e}^{-\mathrm{i}\tau/2}\cos^2\varphi+\mathrm{e}^{\mathrm{i}\tau/2}\sin^2\varphi & -\mathrm{i}\cdot\sin(\tau/2)\sin 2\varphi\\ -\mathrm{i}\cdot\sin(\frac{\tau}{2})\sin 2\varphi & \mathrm{e}^{-\mathrm{i}\tau/2}\sin^2\varphi+\mathrm{e}^{\mathrm{i}\tau/2}\cos^2\varphi\end{pmatrix} \tag{2}$$

where φ is the angle between the crystal axis and the

horizontal direction. In order to encode S_3 component individually by the EOM, we set $\varphi = 45°$. τ is the accumulated phase retardation of two crystals. Thus, the Eq. (2) is simplified as

$$\boldsymbol{P}_{\mathrm{EOM}} = \begin{pmatrix} \cos(\tau/2) & -\mathrm{i}\cdot\sin(\tau/2) \\ -\mathrm{i}\cdot\sin(\tau/2) & \cos(\tau/2) \end{pmatrix} \tag{3}$$

The polarized light after the joint modulator can be written as follows

$$\boldsymbol{E}_o = \boldsymbol{P}_{\mathrm{EOM}} \cdot \boldsymbol{P}_{\mathrm{MOM}} \cdot \boldsymbol{E}_i \tag{4}$$

Applying the relationship between Jones vectors and Stokes vector, the Stokes component of $\boldsymbol{E}_o$ can be described as:

$$\begin{aligned} S_1' &= \boldsymbol{E}_o^+ \boldsymbol{\sigma}_1 \boldsymbol{E}_o = E_x^2 \cos 2\theta \cos\tau \\ S_2' &= \boldsymbol{E}_o^+ \boldsymbol{\sigma}_2 \boldsymbol{E}_o = E_x^2 \sin 2\theta \\ S_3' &= \boldsymbol{E}_o^+ \boldsymbol{\sigma}_3 \boldsymbol{E}_o = E_x^2 \cos 2\theta \sin\tau \end{aligned} \tag{5}$$

where $\boldsymbol{\sigma}_1 = \begin{pmatrix} 1 & 0 \\ 0 & -1 \end{pmatrix}$, $\boldsymbol{\sigma}_2 = \begin{pmatrix} 0 & 1 \\ 1 & 0 \end{pmatrix}$, $\boldsymbol{\sigma}_3 = \begin{pmatrix} 0 & i \\ -i & 0 \end{pmatrix}$ are Pauli matrix, which satisfy above relationship, so the coding process can be mapped to Poincare sphere shown in Fig. 3. Because any complete polarized state of light can be represented as a point on the Poincare sphere, the transformation between points on the sphere represents the change of polarization state. In other words, the encoding of signal light can be achieved by transferring the polarization state on Poincare sphere.

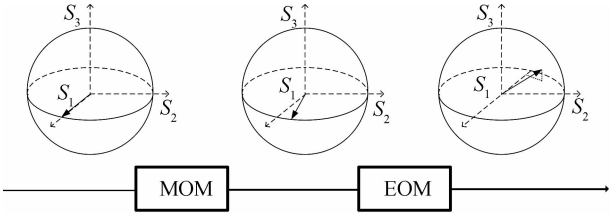

Fig. 3 Poincare sphere

In order to facilitate the measurement and correction, we usually select S_2 and S_3 orthogonal base as components of intrinsic and signal respectively in the single beam of coherent optical communication. The intrinsic component is much larger than the signal component, so the signal light is modulated, and its quantum effect is obvious when signal light intensity is decreased to several hundred photons, and the relation between S_2 and S_3 satisfies: $\Delta S_2 \Delta S_3 \geqslant |\langle S_1 \rangle|$, which is known as Heisenburg uncertainty relation. Therefore, S_2 or S_3 can be randomly selected in QKD.

2.1 Encoding of S_2

In order to encode S_2 component independently, a $\lambda/4$ wave plate (QWP) following to the MOM is added. According to the transformation of matrix optics [13], the transform matrix of QWP is described as

$$\boldsymbol{M}_{\mathrm{QWP}} = \begin{pmatrix} 0 & 0 & 1 \\ 0 & 1 & 0 \\ -1 & 0 & 0 \end{pmatrix} \tag{6}$$

The polarized light I_1 would change into $I_1 = M_{\mathrm{QWP}} \cdot E_0$ after passes through the QWP. Combining with Eq. (5) and (6), the polarized light is presented as

$$\begin{pmatrix} S_1 \\ S_2 \\ S_3 \end{pmatrix} = E_x^2 \begin{pmatrix} \cos 2\theta \sin\tau \\ \sin 2\theta \\ -\cos 2\theta \cos\tau \end{pmatrix} \tag{7}$$

where the MOM has little effect on the angle θ ($-5° < \theta < 5°$), and phase retardance τ in EOM is closed to π, so in Eq. (7): $\sin 2\theta \to 0$, $-\cos 2\theta \cos\tau \to 1$, where $\to$ means approaching, The result show that the point of polarization state of incident light, through the QWP, moves to the top region of the Poincare Sphere , which is shown in Fig. 2. It indicates that the polarized light's S_3 component is much larger than S_2 component. So we consider the S_3 component to be the intrinsic light and the S_2 component to be a signal light in the continuous variable coherent communication, S_2 is modulated by MOM and QWP.

2.2 Encoding of S_3

In the same way, in order to encode S_3 components independently, a Half-Wave Plate (HWP) replaces the QWP in Fig 2, the HWP is described as follows

$$\boldsymbol{M}_{\mathrm{HWP}} = \begin{pmatrix} 0 & 1 & 0 \\ 1 & 0 & 0 \\ 0 & 0 & -1 \end{pmatrix} \tag{8}$$

The polarized light I_2 then can be changed by $I_2 = \boldsymbol{M}_{\mathrm{HWP}} \boldsymbol{E}_0$, combining with Eqs. (5) and (8), the polarized light is presented by

$$\begin{pmatrix} S_1 \\ S_2 \\ S_3 \end{pmatrix} = E_x^2 \begin{pmatrix} \sin 2\theta \\ \cos 2\theta \cos\tau \\ -\cos 2\theta \sin\tau \end{pmatrix} \tag{9}$$

The rotation angle θ of the MOM varies from $-5°$ to $5°$, and phase retardance τ in EOM is closed to π, so in Eq. (9), $\sin 2\theta \to 0$, $\cos 2\theta \sin\tau \to 1$, $-\cos 2\theta \cos\tau \to 0$. The result show that polarization state of incident light can be rotated to the side region (near S_3) of the Poincare sphere. It indicates that the intensity of S_2 component is much larger than that of S_3 component. Therefore, we consider the component S_2 as local oscillator light and the component S_3 as a signal light in the continuous variable coherent communication, and S_3 is encoded by controlling the voltage of the EOM.

3 Design of hardware

3.1 The driving of MOM

Section 2 shows that S_2 and S_3 are encoded by the modulation of MOM and EOM. According to Faraday effect, the polarization direction changes when linearly polarized light propagate along magnetic field within a homogeneous and isotropic medium. Magnetic induction density is proportional to the excitation current. The expression is shown as follows

$$\theta = VBL = VL \frac{N i_0 \mu_0}{l_{\mathrm{gas}}} \tag{10}$$

Where θ is the rotation angle of polarized light; V which is related to Material is Verdet constant; B is magnetic induction intensity; L is the distance passed through the crystal. S_2 is encoded by magnetic induction density, which is proportional to the product of excitation coil number and excitation current. Our solenoid has been tested in 5 times (as shown in Fig. 4) by manufacturer. It is shown that the magnetic induction intensity of the solenoid is linearly relative to the excitation current when the excitation current is at range of 0.4 A to 2 A.

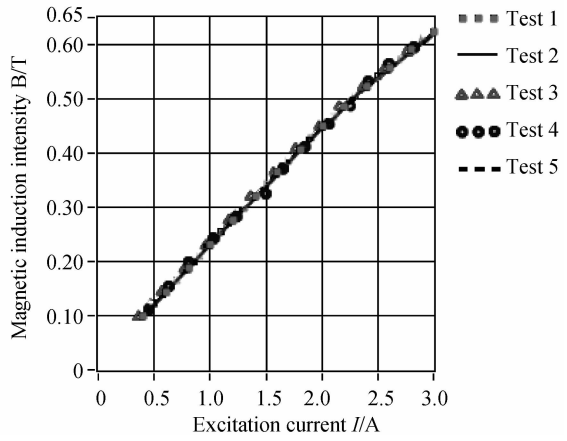

Fig. 4 The characteristic curve of the solenoid

Therefore, we design a current source circuit of range from 0.4 A to 2 A, which adjusts the current of MOM and encodes S_2. The driving circuit is showed in Fig. 5.

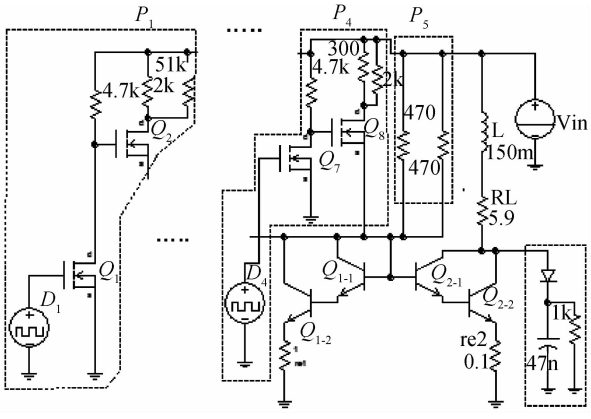

Fig. 5 The driving circuit of MOM

It is controlled by a step driver which is beneficial to heat dissipation and improvement of driving current. The dotted blocks P_1, P_2, P_3, P_4 are driving units. D_1, D_2, D_3, D_4 are affected by a switching digital level and the current are changed progressively by a match resistance at drain side in $Q_1 \sim Q_4$. At last, current source which consists of $Q_{1\text{-}1}$, $Q_{1\text{-}2}$, $Q_{1\text{-}3}$, $Q_{1\text{-}4}$ magnifies the output current. The formula is shown as follow

$$i_1 = ((1-D_1)2^{1-D_1} + (1-D_2)2^{2(1-D_2)} + (1-D_3)2^{3(1-D_3)} + (1-D_4)2^{4(1-D_4)})\Delta i + i_0 \quad (11)$$

where $D_i (i=1,2,3,4)=0,1$. $D_i=0$ indicates digital level is low. $D_i=1$ indicates digital level is high. i_0 is the static current. At last, encoding S_2 can be accomplished by Personal Computer (PC) which connects to $D_1 \sim D_4$ by DAQ Card (Data Acquisition Card) PCI6111E.

3.2 The drive of EOM

In Section 2, it is shown that S_2 and S_3 are modulated by MOM and EOM, respectively, as illustrated in Fig. 3. The EOM 4102M consists of two orthogonal $LiNbO_3$ crystals which acts as phase delay adjustable wave plates as Fig. 6 shows, position of them in space is opposite.

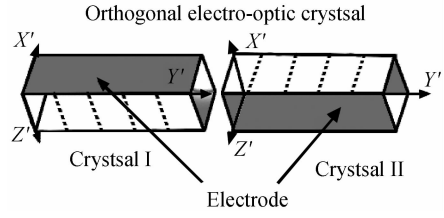

Fig. 6 Structure of EOM

According to the Eq. (9), the S_3 can be encoded independently by EOM. The EOM is modulated by the voltage on electrode as shown in Fig. 6. The driver of EOM is Model 3363B, which integrates driving circuit and its inputs come from DAQ Card.

3.3 The random number generating circuit

Random numbers are necessary for encoding S_2 and S_3, which are generated by hardware and their advantages are easily programming and high-safety. Here, we choose STM32F407 microcontroller as random number generator (RNG shown in Fig. 7) based on a continuous analog noise, which provides a random 32-bit value to the host when reading process occurs. To run the RNG, we just enable the interrupt and set RNGEN bit in the RNG_CR register.

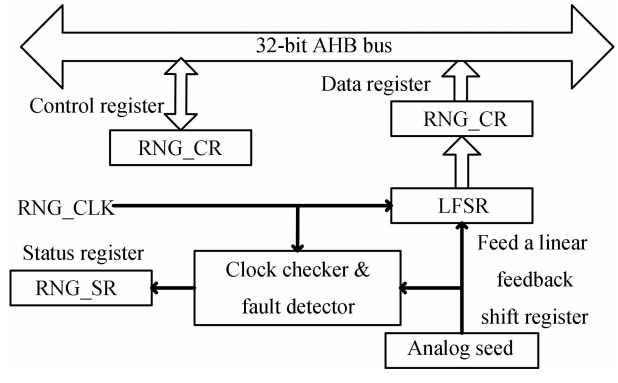

Fig. 7 Generator module of random number

4 Experiment and analysis

4.1 Principle of detecting and experiment

In order to verify the coding scheme, a homodyne detection system is designed, as shown in Fig. 8.

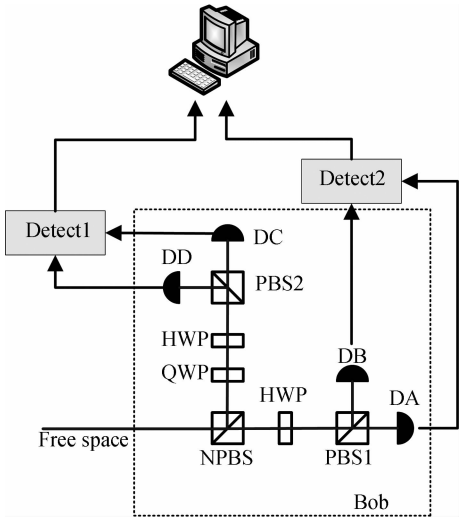

Fig. 8 Diagram of homodyne detection system

The NPBS divides one polarized light beam into two orthogonal light beams. One is to measure S_2, the other is to measure S_3. By analysis, the Detect 1 from the light intensity difference of DA and DB can be presented as

$$I_2 = \frac{1}{2}(S_1 \cos 4\theta + S_2 \sin 4\theta) \tag{12}$$

where θ is the angle between fast axis of HWP and horizontal direction. From Eq. (12), we can work out that S_2 is measured when $\theta = \pi/8$, i. e. $\cos 4\theta = 0$ and $\sin 4\theta = 1$.

In the same way, the Detect 2 from the light intensity difference of DC and DD can be presented as

$$I_3 = \frac{1}{2}(S_2 \cos^2 2\varphi + S_1 \cos 2\varphi \sin 2\varphi + S_3 \sin 2\varphi) \tag{13}$$

φ is the angle between the fast axis of QWP and horizontal component of light. We can work out that S_3 is measured when $\varphi = \pi/4$. Analysis indicates that we can detect S_2 or S_3 by detecting optical intensity, and convert light to voltage. For more details on detecting circuit and principle, see Ref. [14].

Based on the above theories, we assemble a transmitting and acquiring system (as shown in Fig. 9) to verify our scheme in atmospheric environment. The structure of light path in Fig. 9 is the same as that in Fig 2. Firstly, random numbers generated by STM32F407 are collected. Then the MOM and EOM are driven to send signal at rate 3bps. Over a distance of 2 meters, the beam propagates to the receiving terminal. Because the distance is very short, the atmospheric polarization noise can be ignored. At last, photoelectric converter sends the voltage signal to data acquisition (DAQ) card (PCI6111E) at a sampling rate of 1 kHz.

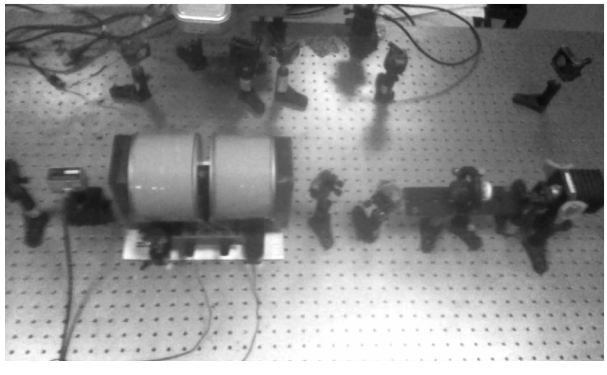

Fig. 9 The photo of system

4.2 Analysis of results

During the experiment, S_2 or S_3 is encoded randomly, and we get measurement results shown in Fig. 10 and Fig. 11. When S_2 is encoded in binary mode which comes from microcontroller STM32F407, the MOM is modulated. By comparing the sending data with the receiving data in Fig. 10, it is observed they are basically identical.

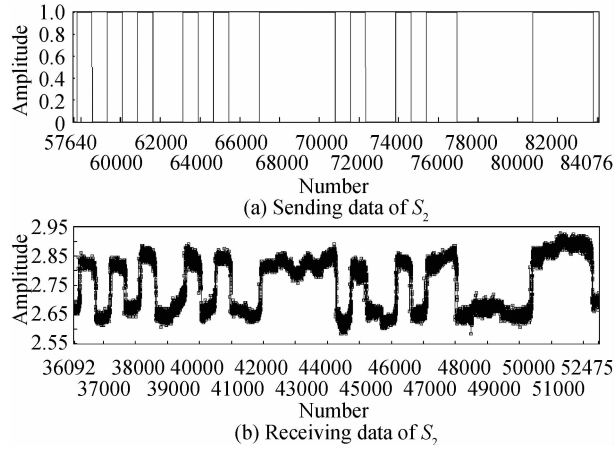

Fig. 10 Comparison of sending data and receiving data

Similarly, when S_3 is encoded in binary mode, the EOM is modulated, and the sending data and receiving data are basically identical, too.

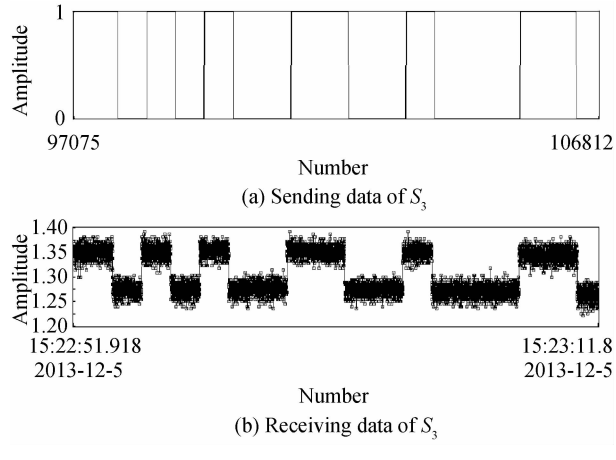

Fig. 11 Comparison of sending data and receiving data

To acquire a reasonable consequence, it is necessary to take consideration of noise which is classified into three categories: 1) The stability of driver power and variance of each device. 2) The

electromagnetic disturbance comes from amplifier circuit of photoelectric converter. 3) The existence of optical noise and crosstalk ambient light. They are mainly manifested as a thick ribbon (as shown in Fig. 10 and Fig. 11). In order to get a statistical analysis, the receiving data is processed as: a) A threshold is defined by nearby data which is extracted from previous data. b) Compare with threshold, if the new data are greater than the threshold, they are classified as "1", Otherwise, they are classified as "0". Thus, the useful information can be extracted and the noise is removed, then the Bit Error Rate (BER) can be calculated, the procedure of LabVIEW is shown in Fig. 12.

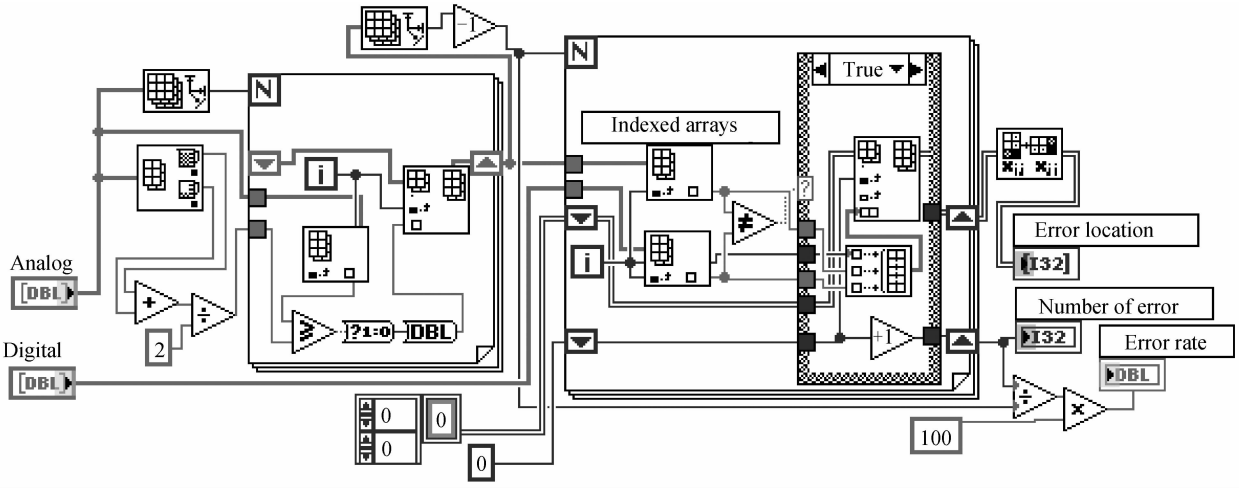

Fig. 12 Control flow chart by LabVIEWg EA

The primary results show that BER of MOM is 2.18%, and EOM is 3.56%. Elser has reported similar experimental results, the BER changes within a range of 1% to 10% at postselection threshold[7]. That is to say, our experimental results has reached a higher level, the scheme of joint modulation is feasible for CVQKD.

Since CVQKD is essentially different with the conventional optical communication, In CVQKD, In addition to the errors in classical channel, there is two effects in CVQKD: 1) a very weak quantum of signal to noise ratio is relatively low, 2) there is quantum effect on the characteristics of quantum signal at the same time, Stokes parameters satisfy with the uncertainty relation between the operators, but it also brings in quantum noise[12], so the total BER is greater than the one in classical communication. Therefore, it is necessary to process the experimental data further, including data reconciliation and privacy amplification process.

5 Conclusion

In this paper, we has proposed a coding scheme of joint modulation including magneto-optic modulation and electro-optic modulation for single-beam continuous variable coherent optical communication. The coding principle of the joint modulator is analyzed in Stokes matrix theory. A communication and detection system is setup for demonstrating our scheme. Also we program a LabVIEW procedure to control data acquisition and analyze collected data. The primary results show that when S_2 or S_3 is randomly selected as QKD, the receiving data is almost consistent with sending data, the BER for magneto-optic modulating is 2.18%, for electro-optic modulating is 3.56%. It can be applied in single-beam CVQKD.

Reference

[1] CAO Ya-mei, NIE Min, LIU Xiao-hui. Differential phase encoding scheme for the polarization state of quantum signaling and simulation[J]. *Acta Photonica Sinica*, 2013, **42**(6): 721-726.

[2] YUAN Su-zhen, XUN Zhi-fu, TIAN Jun-long. Quantum secret sharing scheme with N-ordered entangled photon pairs[J]. *Acta Photonica Sinica*, 2011, **40**(8): 1248-1252.

[3] ZHOU Wu-lin, HUANG Chun-hui. Continuous variable phase detection system based on LabVIEW[J]. *Acta Photonica Sinica*, 2011, **40**(5): 785-788.

[4] HUANG Chun-hui, RONG Wei-bo. A control scheme of polarization generator based on three LiNbO3 wave plates[J]. *Laser & Optoelectronics Progress*, 2013, **50**(5): 0523031-0523037.

[5] ULRIK L, CHRISTINE S, GERD L, *et al*. Continuous variable Quantum Information Processing[J]. *Laser & Photonics Reviews*, 2010, **4**(3): 337-354.

[6] JOUGUET P, KUNZ S, LEVERRIER A, *et al*. Experimental demonstration of log-distance continuous variable quantum key distribution[J]. *Nature Photonics*, 2013, **7**(5): 378- 371.

[7] GROSSHANS F, VANASSCHE G, WENGER J, *et al*. Quantum key distribution using gaussian modulated coherent states[J]. *Quantum Physics*, 2003, **3**(2): 238-241.

[8] LALOE F, MULLIN W. Quantum properties of a single beam splitter[J]. *Foundations of Physics*, 2012, **42**(1): 53-67.

[9] BARTLEY T. Enhanced free space beam capture by improved optical tapers[M]. HEIM B, ELSER D. 1rd ed. Germany: Springer Berlin Heidelberg, 2010: 100-107.

[10] ELSER D, BARTLEY T, HEIM B, *et al*. Feasibility of free space quantum key distribution with coherent polarization states[J]. *New Journal of Physics*, 2009, **11**(4): 14-26.

[11] TAO Chun-kan, TAO Kuang. Optical information theory [M]. 1rd . Beijing: Science Press, 1999: 119-126.

[12] WAN Qing, HUANG Chun-hui. A novel Stokes parameters encoding scheme for free-space coherent optical communication [J]. *Frontierse of Optoelectronices*, 2012, **5**(2): 231-236.

[13] YAN Ji-xiang. Matrix optics [M]. WEI Guang-hui. 1rd. Beijing: Weapons Industry Press, 1995: 177-203.

[14] CHEN Chu, HUANG Chun-hui. Improved version of coherent light detection system design[J]. *Laser & Infrared*, 2008, **38**(6): 580-582.